Generalized $\vec{k}\cdot\vec{p}$ interpolation method for electronic band structure: bcc iron

H. J. F. Jansen
Materials Science Center, Solid State Physics Laboratory, University of Groningen, Groningen, The Netherlands

F. M. Mueller
Research Institute for Materials, University of Nijmegen, Toernooiveld, Nijmegen, The Netherlands

(Received 2 April 1979)

We have developed a series of $\vec{k}$-dependent model band Hamiltonians in symmetrized polynomials, centered at points of high symmetry in the Brillouin zone, by means of local-group-invariant projectors — similar to the familiar Clebsh-Gordan coefficients of the full rotation group. We have tested these ideas by applying them to bcc iron. The results show that electronic structure is exponentially convergent in the expansion order of the polynomials: Expanding to fourth-order model energy bands fit Korringa-Kohn-Rostoker (KKR) bands to better than 2 mRy. For the bands of interest, the model scheme was more than 200 times faster than a fast KKR scheme.

I. INTRODUCTION

The application of model-Hamiltonian schemes to problems in physics has been both extensive and intensive. In the case of the band problem, one of the earliest of such applications was the $\vec{k}\cdot\vec{p}$ method, based on perturbation theory.[1] Generally this technique has been restricted to considering the electronic structure of semiconductors or semimetals for which only a few bands, local in $\vec{k}$ space, were of interest.[2] The $\vec{k}\cdot\vec{p}$ method forms a convenient and simple scheme to interpolate both energy and wave functions.

For general materials, theorists have applied other methods, such as pseudopotentials,[3] parametrized tight-binding or Slater-Koster method,[4] or combined schemes.[5] Alternatively much of recent effort in band theory has focused on techniques to speed up first-principles methods to make them comparable with model-Hamiltonian methods. Since, however, there will always be problems in which the effects of a few bands out of many dominate the physics, it is clear that the smaller secular matrices available in model Hamiltonians will always have their use.

In this paper we reexamine the idea of $\vec{k}\cdot\vec{p}$-like model Hamiltonians, $\hat{H}(\vec{k})$, which approximate the energy-band structure in a series of polynomial expansions about selected high-symmetry points, $\vec{K}_i$. By binding the expansions to high-symmetry points, we preserve, of course, local-point-group symmetry: the polynomial expansion coefficients are symmetry restricted by the transformation properties of the underlying reciprocal lattice and band structure. The utility of our method will depend on the rate of convergence of the local Hamiltonians as a function of both the order of the polynomial set and the radius of the domain of each $\hat{H}(\vec{k})$. To test the ideas we have made an application to a new Korringa-Kohn-Rostoker (KKR) band structure of nonmagnetic bcc iron calculated from Wood's 1962 potential.[6] The results show that fourth-order expansions, made about the four high-symmetry points, are sufficient to produce energy bands to within an accuracy of 2 mRy or of order 1% of the d-band width.

The plan of this paper is as follows: Sec. II discusses the formal development of the theory, Sec. III the results, and Sec. IV draws our conclusions.

II. FORMAL DEVELOPMENT OF $\vec{k}\cdot\vec{p}$ MODEL HAMILTONIAN

In considering local expansions, it is natural to rely on the $\vec{k}\cdot\vec{p}$ method. Schrödinger's equation then takes the following well-known form[1]:

$$\sum_m H_{nm}(\vec{k})C_m(\vec{k}) = E(\vec{k})C_n(\vec{k}) \quad , \tag{1}$$

where the matrix elements $H_{nm}(\vec{k})$ may be constructed, using a complete set[1] of Kohn-Luttinger basis functions, $\psi_n(\vec{k},\vec{r})$, as

$$H_{nm}(\vec{k}) = \int d^3r\, \psi_n^*(\vec{K},\vec{r})[-\Delta + 2(\vec{k}-\vec{K})\cdot\vec{p} + (\vec{k}-\vec{K})^2 + V(\vec{r})]\psi_m(\vec{K},\vec{r}) \quad . \tag{2}$$

The diagonal terms have the simple form

$$E_n(\vec{K}) + (\vec{k}-\vec{K})^2 + \vec{p}_{nn}\cdot(\vec{k}-\vec{K}) \quad ;$$

the off-diagonal terms contain only linear expressions $\vec{k}\cdot\vec{p}_{nm}$. Here we have defined $\vec{p}_{nm}$ to be

$$\vec{p}_{nm} = \int d^3r\, \psi_n^*(\vec{K},\vec{r})\,\vec{p}\,\psi_m(\vec{K},\vec{r}) \quad . \tag{3}$$

$\vec{p}_{nm}$ is nonzero only if the states n and m can be coupled through an operator of angular momentum one. $\vec{p}_{nn}$ is zero when the group of $\vec{K}$ contains the inversion operator.

We now want to restrict Eq. (1) to a small set of levels near, for example, the Fermi energy. This can be done using Löwdin perturbation theory.[1] We construct the matrix

$$U_{nm}(\vec{k},E)=H_{nm}(\vec{k})+\sum_{\alpha}{}'\frac{H_{n\alpha}(\vec{k})H_{\alpha m}(\vec{k})}{E-H_{\alpha\alpha}(\vec{k})}+\sum_{\alpha\neq\beta}{}'\frac{H_{n\alpha}(\vec{k})H_{\alpha\beta}(\vec{k})H_{\beta m}(\vec{k})}{[E-H_{\alpha\alpha}(\vec{k})][E-H_{\beta\beta}(\vec{k})]}+\cdots . \tag{4}$$

n and m belong to our small set of interesting levels. The prime denotes summation outside the selected set. The model Hamiltonian will be used only over a finite range of energies: hence we can, as usual, replace E in Eq. (4) by an average energy $\bar{E}$ with negligible error. Note also that by construction $U_{nm}(\vec{k},\bar{E})$ obeys the same transformation properties as $H_{nm}(\vec{k})$. We then solve the eigenvalue problem $U(\vec{k},\bar{E})c=Ec$, in order to find the energy levels $E^j(\vec{k})$ and the eigenvectors at each point $\vec{k}$.

Making a polynomial expansion of U in terms of the components $\vec{k}-\vec{K}$, it is easy to see that the first term contributes only to the orders 0, 1, and 2. The second term contributes to the orders 2, 3, 4, $\cdots$ and the nth term has no contributions to lower orders than n. The polynomials we use are basis functions for irreducible representations of the group of $\vec{K}$. When $\vec{K}$ has cubical symmetry they are just Kubic harmonics, multiplied by an even power of k. It is possible to reorder the expansion (4) in the following way:

$$U_{nm}(\vec{k},\bar{E})=\sum_{\alpha ij}A_{nm}^{\alpha ij}(\bar{E})P_{\alpha ij}(\vec{k}-\vec{K}) . \tag{5}$$

$P_{\alpha ij}(\vec{k})$ is a polynomial belonging to the ith row of the jth representation α of the group of $\vec{K}$. The coefficients A are determined by a general form of the Wigner-Eckart theorem. This is caused by the fact that a nth order term couples states through $(\Gamma_{15})^n$. They can be written as a product of a generalized Clebsch-Gordan coefficient and a reduced matrix element. This structure is similar to that used to determine the symmetry of model-Hamiltonian matrix elements in the Slater-Koster scheme.[4] Because we have chosen our point $\vec{K}$ to be a high-symmetry point, many of the coefficients are zero, dictated by symmetry; others are equal. This substantially reduces the number of necessary parameters for a given order.

Expression (5) can now be used to construct model Hamiltonians. We simply use the reduced matrix elements as energy-independent adjustable parameters. Also we truncate the series (5) at some order M of $(\vec{k}-\vec{K})$. In this way it is clear that our scheme can be used only in a limited energy range. Looking at Eq. (4) we see that the variation in energy E must be small compared to the difference $E-E'$, where E' denotes the energy of the nearest level not represented within the model Hamiltonian. The interaction with core levels appears to be negligible.

III. RESULTS USING KKR BANDS OF bcc IRON

As a test case we used a KKR band-structure calculation, based on the potential given by Wood[6] and

TABLE I. Energy levels fitted at four high-symmetry points.

	Γ	H	P	N
Highest core	−2.79 (Γ_{15})	−2.82 (H_{15})	−2.81 (P_4)	−2.79 (N_4')
	0.096 (Γ_1)			0.395 (N_1)
		0.413 (H_{12})	0.539 (P_4)	0.542 (N_2)
Conduction band	0.641 (Γ_{25}')			0.754 (N_1')
				0.763 (N_1)
	0.763 (Γ_{12})	0.850 (H_{25}')	0.786 (P_3)	0.783 (N_4)
				0.873 (N_3)
First unused higher level	2.65 (Γ_{25})	1.476 (H_{15})	1.401 (P_4)	1.331 (N_1)
Size of model Hamiltonian	6×6	5×5	5×5	6×6
Local region parameter r_n	0.71	0.58	0.41	0.38

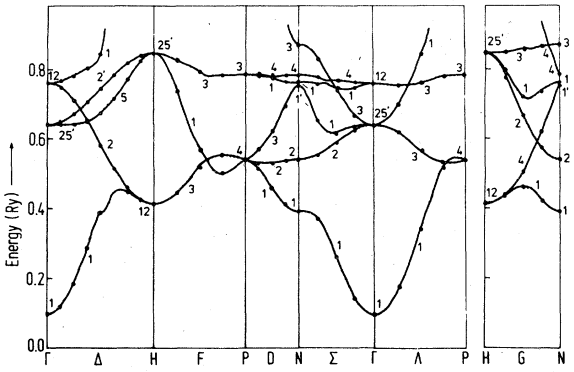

FIG. 1. Energy bands of bcc iron along high-symmetry directions. The solid dots are KKR bands; the solid lines were produced by the $\vec{k}\cdot\vec{p}$ scheme. The fit is quite close reflecting the overall 2 mRy error.

a lattice parameter $a = 5.4057$ (a.u.). Although this calculation is old by current standards, his Table IV allowed us a simple confirmation of the (new) KKR bands. The main part of his table is correct within some 7 mRy. Beside three typing errors [(1,7,0) band 1 should be 0.432; (3,5,1) band 5 should be 0.829; (3,3,2) band 3 should be 0.598] there is a systematic difference in the structure associated with the Γ_1 level. Our values are lower by about 20 mRy. A possible cause could be that in Wood's calculation the mesh for the radial integration near zero was not fine enough, introducing errors mainly in the $l=0$ parts.[7] Our KKR results were converged to better than 2 mRy.

Table I lists the levels we have used for our expansions around the points Γ, H, P, and N. In Fig. 1 the band structure is displayed along the lines of high symmetry (dotted points). The calculation was done at 55 points in the irreducible wedge of the Brillouin zone (a "$\pi/4a$" mesh). Comparing this band structure to Callway's,[8] we find that we are in close agreement.[9,10] We have changed our representations along the D and G lines to be more compatible with N.

The size of the several model-Hamiltonian matrices is governed by the band structure around the high-

TABLE II. Product representations of Γ.

	Γ_1	Γ'_{25}	Γ_{12}
Γ_1	Γ_1	Γ'_{25}	Γ_{12}
Γ'_{25}	Γ'_{25}	$\Gamma_1+\Gamma_{12}+\Gamma'_{15}+\Gamma'_{25}$	$\Gamma'_{15}+\Gamma'_{25}$
Γ_{12}	Γ_{12}	$\Gamma'_{15}+\Gamma'_{25}$	$\Gamma_1+\Gamma_2+\Gamma_{12}$

TABLE III. Product representations of H.

	H_{12}	H'_{25}
H_{12}	$H_1+H_2+H_{12}$	$H'_{15}+H'_{25}$
H'_{25}	$H'_{15}+H'_{25}$	$H_1+H_{12}+H'_{15}+H'_{25}$

symmetry points. For Γ and N we used 6×6 matrices, for H and P 5×5 matrices. These choices were sufficient but not necessary ones, and were dictated by convenience. We were interested that our model Hamiltonian only fit in the $3d$-band neighborhood of the Fermi energy. Group theory furnishes us the representations α which appear in the matrices. (See Tables II–V for this reduction in the Appendix.) Detailed information we can, of course, obtain only from the Clebsch-Gordan coefficients. With their aid it is possible to construct the matrix elements. A list of the number of adjustable parameters is given in Table VI. Fits up to fourth order in $\vec{k}-\vec{K}$ around Γ, H, and P needed only about 30 parameters. Numerically this problem can be handled using a Marquardt algorithm.[11] The low symmetry of the N point dictated that a fourth-order fit would involve an excessive number of free parameters. We have therefore used a lower-order fit around N and correspondingly shrunk that region. In addition we have used some sixth-order parameters at H and Γ.[12]

For each of the high-symmetry points the 55 k points were ordered in increasing distance to $\vec{K}$. We then determine the parameters in such a way that they gave the best approximation to the energy values of the first n points. Then the rms error of the fit was calculated and also the distance r_n of the point $\vec{k}_n$ to $\vec{K}$. (r_n is the radius of the region that is covered by the fitting scheme.) The results are given in Fig. 2, order meaning the highest power of $\vec{k}-\vec{K}$ used in the expansions. These data suggest that for a given order the rms error is an exponentially increasing function of the distance, covered by the fit. Also for a given finite region the rms error *decreases* ex-

TABLE IV. Product representations of P.

	P_3	P_4
P_3	$P_1+P_2+P_3$	P_4+P_5
P_4	P_4+P_5	$P_1+P_3+P_4+P_5$

TABLE V. Product representations of N.

	N_1	N_2	N_3	N_4	N_1'
N_1	N_1	N_2	N_3	N_4	N_1'
N_2	N_2	N_1	N_4	N_3	N_2'
N_3	N_3	N_4	N_1	N_2	N_3'
N_4	N_4	N_3	N_2	N_1	N_4'
N_1'	N_1'	N_2'	N_3'	N_4'	N_1

ponentially as a function of order. As seen from Table VI the number of symmetry independent parameters increases as the square of the order, with the N point having the largest number per order. At Γ we have the greatest accuracy; the accuracy at H is less, although the point symmetry is the same as at Γ. This is a reflection of the presence of the level H_{15}, which is relatively near, and our desire for small matrices. At P and N the situation is worse, because there the symmetry is even lower.

One can hope to get better fits by concentrating all effort on E_F, the Fermi energy. This idea was tested by introducing weight factors $\exp\{-\gamma[E_F - E(\vec{k})]^2\}$. However, the overall fit was then much worse, because energy values which can be fitted least well dominated the structure. Our final results show on a band by band basis an error independent of energy.

We have separately considered model Hamiltonians about four high-symmetry points. In order to use our scheme we need, of course, to be able to move smoothly throughout the Brillouin zone. In principle it would be possible to employ a single expansion

TABLE VI. Number of symmetry-independent parameters as a function of order for the bcc high-symmetry points.

order	Γ	H	P	N
0	3	2	2	6
1	0	0	2	4
2	9	6	6	30
3	0	0	7	13
4	19	13	13	69

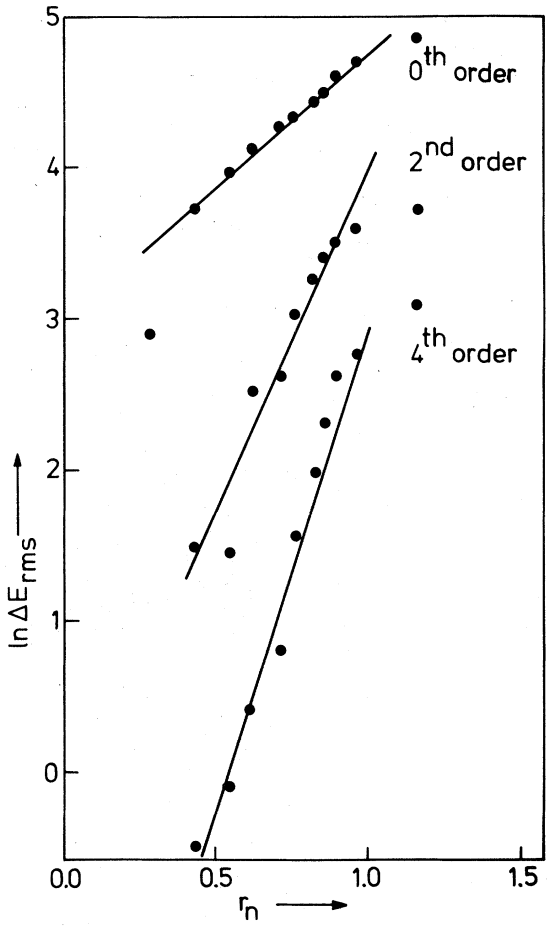

FIG. 2. Logarithm of best rms fitting error (in mRy) around Γ as a function of the radius r_n of the included initial $\vec{k}$ points, and as a function of the order of the highest polynomial used the $\vec{k}\cdot\vec{p}$ scheme. H is at 1.16 a.u. For a fixed radius the error decreases exponentially as a function of order.

point — Γ for example — and derive everything from that one expansion. In practice this involves too many bands and parameters to be convenient. The $\vec{k}\cdot\vec{p}$ idea looses simplicity.

After some experimentation we found that Gaussian interpolation between the points worked well: the Gaussian function cuts off the expansions faster than the exponentially growing errors. It is possible to extend the sum over four high-symmetry points from the $\frac{1}{48}$th of the zone used in Eq. (6) to sums over several high-symmetry points of one zone or over multiple high-symmetry points in extended zones. In practice we have found that such extensions were not necessary. The partial fits are combined to one global fit in the following way:

$$\tilde{E}^j(\vec{k}) = \frac{\sum_{\vec{K}}\{\exp[-\alpha(\vec{k}-\vec{K})^2/r^2(\vec{K})]E^j(\vec{K},\vec{k})\}}{\sum_{\vec{K}}\exp[-\alpha(\vec{k}-\vec{K})^2/r^2(\vec{K})]} \quad (6)$$

$r(\vec{K})$ is a radius of a sphere around $\vec{K}$. α can be chosen freely, to give an optimal result. We restrict ourselves to energy values lower than 0.9 Ry. We found that $\alpha = 10$ gave an overall optimal fit for bcc iron, using the r's in Table I.

In Fig. 1 we present the initial set of bcc Fe bands along high-symmetry lines as dots and the global fitted bands from expansion (6) as lines. The overall agreement is quite good, reflecting the overall 2 mRy rms error. The lowest band along Γ to H exhibits one of the largest errors of the scheme. This is due to the fact that the midpoint along Δ from Γ to H is the furthest from any of the chosen expansion points and the lowest Δ_1 band has large width and strong curvature in the neighborhood of H. Such a region can be easily repaired by the addition of selected parameters: we have preserved this error in Fig. 1 to remind the reader that *derivatives* have one higher order of error than bands themselves, and that our $\vec{k}\cdot\vec{p}$ method does suffer somewhat in the "joining" regions along symmetry lines. The addition of one more diagonal Γ parameter makes the Γ_1 fitting error invisible.

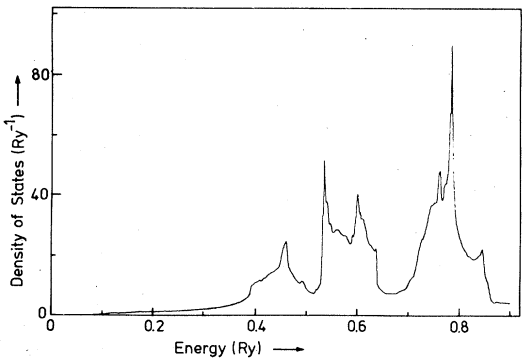

FIG. 3. Density of states of paramagnetic bcc iron. The structure is similar to that of Ref. 13.

As an application of the scheme we present in Fig. 3 the density of states of paramagnetic bcc iron calculated from the scheme and using a linear tetrahedron method. We have used 1500 tetrahedrons in $\frac{1}{48}$th of the Brillouin zone. The structure is similar to that calculated by Moruzzi, Janak, and Williams.[13]

IV. DISCUSSION AND CONCLUSION

The generalized $\vec{k}\cdot\vec{p}$ method forms a convenient and simple means to interpolate electronic structure. By fitting larger and larger neighborhoods of the high-symmetry points the parameters can be sequentially developed in orders. Then one can make better fits by increasing the order and simultaneously the radius of the region. In this way partial fits are derived in a relatively easy and straight forward way. The combination of partial fits into one global fit is also simple. The resultant global fit has its largest errors at $\vec{k}$ points furthest from the high-symmetry points.

For simplicity we have applied our method to a well-known case: bcc Fe. For this case the overall simplicity and speed of the fastest KKR methods is not more than one order of magnitude more costly than the interpolation scheme. On our machine five converged bands took 8 seconds per $\vec{k}$ point by KKR, whereas the same five took 0.02 seconds by the $\vec{k}\cdot\vec{p}$ scheme. We anticipate that our ideas will find their greatest application in interpolating the band structure of complex multiatom per unit cell materials. Finally although the applications we have made here depended only on energy, it is clear that properties dependent on wave functions may also be interpolated by means of the same ideas.[14] We hope to return to these in a future publication.

ACKNOWLEDGMENTS

We wish to thank Dr. M. H. Boon, Dr. H. W. Myron, and Drs. A. Th. van Kessel for helpful discussions, and Professor J. Callaway for sending us copies of both his unpublished results and computer codes. This work was supported as part of the research program of the Stichting voor Fundamenteel Onderzoek der Materie (FOM) and received financial support through the Nederlandse Organisatie voor Zuiver Wetenschappelijk Onderzoek (ZWO).

APPENDIX: PARAMETERS, MATRICES, AND TECHNIQUES FOR bcc $\vec{k}\cdot\vec{p}$ MODEL HAMILTONIANS

The $\vec{k}\cdot\vec{p}$ techniques we have derived will, of course, work for every lattice. Since the band struc-

TABLE VII. Symmetry adapted polynomials (Γ centered) up to fourth order.

Γ_1: 1; r^2; r^4; $x^4+y^4+z^4$;
Γ_2: —
Γ_{12}: $(x^2-y^2)3^{1/2}$, $3z^2-r^2$; $(x^2-y^2)r^2 3^{1/2}$, $(3z^2-r^2)r^2$; $(x^4-y^4)3^{1/2}$, $2z^4-x^4-y^4$;
Γ_{15}: x,y,z; xr^2, yr^2, zr^2; x^3, y^3, z^3;
Γ_{25}: $z(x^2-y^2), x(y^2-z^2), y(z^2-x^2)$;
Γ_1': —
Γ_2': xyz;
Γ_{12}': —
Γ_{15}': $xy(x^2-y^2), yz(y^2-z^2), zx(z^2-x^2)$;
Γ_{25}': xy, yz, zx; xyr^2, yzr^2, zxr^2; xyz^2, yzx^2, zxy^2;

ture of bcc transition metals forms an active field of research, we include in this Appendix our explicit results for the interested reader. Further results are available in Ref. 12.

The actual form of the model Hamiltonians can be found in the following way. First we have to decide what levels are important. It appeared to be unnecessary and even undesirable to include the core levels. At Γ the choice is then an obvious one. At H we first tried to incorporate the H_{15} levels, but it turned out to be better not to do so.

Let us illustrate the matrix construction by looking at Γ. The levels of interest here are Γ_1, Γ_{25}', and Γ_{12}. By making a group multiplication table it is easy to see which representations appear (Table II). To find explicit information about the specific rows of the representation we have to look at the generalized Clebsch-Gordan coefficients. Given the representation matrices $D_{ij}^{\alpha}(R)$ they can be calculated, up to a phase factor, from the projector

$$\begin{pmatrix} \alpha & \beta & | & \gamma \\ k' & l' & | & m' \end{pmatrix}^* \begin{pmatrix} a & \beta & | & \gamma \\ k & l & | & m \end{pmatrix} = \frac{n_\gamma}{g} \sum_R D_{k'k}^{\alpha}(R) D_{l'l}^{\beta}(R) D_{m'm}^{\gamma *}(R) . \quad (7)$$

Our matrices were all real. Examples for Γ are given[14] in Tables VII and VIII. We have not included some Γ_{15}' representations to preserve simplicity.

TABLE VIII. Fourth-order matrix, Γ centered.

$(1/1) = c_1 + c_4 r^2 + c_{13} r^4 + c_{14}(x^4+y^4+z^4)$.
$(x^2-y^2/1) = c_5 3^{1/2}(x^2-y^2) + c_{15} 3^{1/2}(x^2-y^2)r^2 + c_{16} 3^{1/2}(x^4-y^4)$.
$(3z^2-r^2/1) = c_5(3z^2-r^2) + c_{15}(3z^2-r^2)r^2 + c_{16}(2z^4-x^4-y^4)$.
$(x^2-y^2/x^2-y^2) = c_2 + c_6 r^2 + c_{17} r^4 + c_{18}(x^4+y^4+z^4) - c_7(3z^2-r^2) - c_{19}(3z^2-r^2)r^2 - c_{20}(2z^4-x^4-y^4)$
$(3z^2-r^2/x^2-y^2) = -c_7 3^{1/2}(x^2-y^2) - c_{19} 3^{1/2}(x^2-y^2)r^2 - c_{20} 3^{1/2}(x^4-y^4)$.
$(3z^2-r^2/3z^2-r^2) = c_2 + c_6 r^2 + c_{17} r^4 + c_{18}(x^4+y^4+z^4) + c_7(3z^2-r^2) + c_{19}(3z^2-r^2)r^s + c_{20}(2z^4-x^4-y^4)$
$(xy/1) = c_8 xy + c_{21} xyr^2 + c_{22} xyz^2$.
$(yz/1) = c_8 yz + c_{21} yzr^2 + c_{22} yzx^2$.
$(zx/1) = c_8 zx + c_{21} zxr^2 + c_{22} zxy^2$.
$(xy/x^2-y^2) = c_{23} xy(x^2-y^2)$.
$(yz/x^2-y^2) = -\frac{1}{2} c_{23} yz(y^2-z^2) + \frac{1}{2} 3^{1/2} c_9 yz + \frac{1}{2} 3^{1/2} c_{24} yzr^2 + \frac{1}{2} 3^{1/2} c_{25} yzx^2$.
$(zx/x^2-y^2) = -\frac{1}{2} c_{23} zx(z^2-x^2) - \frac{1}{2} 3^{1/2} c_9 zx - \frac{1}{2} 3^{1/2} c_{24} zxr^2 - \frac{1}{2} 3^{1/2} c_{25} zxy^2$.
$(xy/3z^2-r^2) = c_9 xy + c_{24} xyr^2 + c_{25} xyz^2$.
$(yz/3z^2-r^2) = -\frac{1}{2} 3^{1/2} c_{23} yz(y^2-z^2) - \frac{1}{2} c_9 yz - \frac{1}{2} c_{24} yzr^2 - \frac{1}{2} c_{25} yzx^2$.
$(zx/3z^2-r^2) = \frac{1}{2} 3^{1/2} c_{23} zx(z^2-x^2) - \frac{1}{2} c_9 zx - \frac{1}{2} c_{24} zxr^2 - \frac{1}{2} c_{25} zxy^2$.
$(xy/xy) = c_3 + c_{10} r^2 + c_{26} r^4 + c_{27}((x^4+y^4+z^4) + c_{11}(3z^2-r^2) + c_{28}(3z^2-r^2)r^2 + c_{29}(2z^4-x^4-y^4)$.
$(yz/xy) = c_{12} zx + c_{30} zxr^2 + c_{31} zxy^2$.
$(zx/xy) = c_{12} yz + c_{30} yzr^2 + c_{31} yzx^2$.
$(yz/yz) = c_3 + c_{10} r^2 + c_{26} r^4 + c_{27}(x^4+y^4+z^4) + c_{11}(3x^2-r^2) + c_{28}(3x^2-r^2)r^2 + c_{29}(2x^4-y^4-z^4)$.
$(zx/yz) = c_{12} xy + c_{30} xyr^2 + c_{31} xyz^2$.
$(zx/zx) = c_3 + c_{10} r^2 + c_{26} r^4 + c_{27}(x^4+y^4+z^4) + c_{11}(3y^2-r^2) + c_{28}(3y^2-r^2)r^2 + c_{29}(2y^4-x^4-z^4)$.

[1]See, for example, J. Callaway, *Quantum Theory of Solids* (Academic, New York, 1974), Parts A and B, and references therein.
[2]E. O. Kane, in *Semi-conductors and Semi-metals,* edited by R. K. Willardson and A. C. Beer (Academic, New York, 1966), Vol. 1.
[3]W. A. Harrison, *Pseudopotentials in the Theory of Metals* (Benjamin, New York, 1966).
[4]J. C. Slater and G. F. Koster, Phys. Rev. 94, 1498 (1954).
[5]F. M. Mueller, Phys. Rev. 153, 659 (1967).
[6]J. H. Wood, Phys. Rev. 126, 517 (1962).
[7]We are grateful to Dr. D. D. Koelling for this suggestion.
[8]J. Callaway and C. S. Wang, Phys. Rev. B 16, 2095 (1977); we have compared our results with the symmetry of their minority-spin states.
[9]R. A. Tawil and J. Callaway, Phys. Rev. B 7, 4242 (1973).
[10]Our group structures mainly follow that of Ref. 1. Some of our D and G representations are different.
[11]D. W. Marquardt, J. Appl. Math. 11, 431 (1963).
[12]H. J. F. Jansen and F. M. Mueller, *BSB Internal Report* (unpublished). Copies of our Fortran codes and parameters are available on request.
[13]V. L. Moruzzi, J. F. Janak, and A. R. Williams, *Calculated Electronic Properties of Metals* (Pergamon, New York, 1978).
[14]Similar formal ideas were discussed by A. J. Hughes, Phys. Rev. 166, 776 (1968), in his treatment of silicon. Hughes has stressed wave functions, we stress model Hamiltonians: our conclusion remains that such schemes work in a rather straightforward way.